The Geological Society of America
Special Paper 553

Parent crater for Australasian tektites beneath the sands of the Alashan Desert, Northwest China: Best candidate ever?

Jiří Mizera
Nuclear Physics Institute, Czech Academy of Sciences, Hlavní 130, 250 68 Husinec-Řež, Czech Republic, and
Institute of Rock Structure and Mechanics, Czech Academy of Sciences, V Holešovičkách 41, 182 09 Praha 8, Czech Republic

Zdeněk Řanda
Václav Suchý
Vladimír Strunga
Nuclear Physics Institute, Czech Academy of Sciences, Hlavní 130, 250 68 Husinec-Řež, Czech Republic

Jaroslav Klokočník
Astronomical Institute, Czech Academy of Sciences, Fričova 298, 251 65 Ondřejov, Czech Republic

Jan Kostelecký
Research Institute of Geodesy, Topography and Cartography, 250 66 Zdiby 98, Czech Republic, and
Faculty of Mining and Geology, VSB-Technical University of Ostrava, 708 33 Ostrava, Czech Republic

Aleš Bezděk
Astronomical Institute, Czech Academy of Sciences, Fričova 298, 251 65 Ondřejov, Czech Republic, and
Faculty of Civil Engineering, Czech Technical University in Prague, 166 29 Praha 6, Czech Republic

Zdeněk Moravec
Faculty of Science, Masaryk University, Kamenice 5, 625 00 Brno, Czech Republic

ABSTRACT

Australasian tektites represent the largest group of tektites on Earth, and their strewn field covers up to one sixth of Earth's surface. After several decades of fruitless quest for a parent crater for Australasian tektites, mostly in the main part of the strewn field in Indochina, the crater remains undiscovered. We elaborate upon a recently suggested original hypothesis for the impact in the Alashan Desert in Northwest China. Evidence from geochemical and isotopic compositions of potential source materials, gravity data, and geographic, paleoenvironmental, and ballistic considerations support a possible impact site in the Badain Jaran part of the Alashan Desert. In further support of an impact location in China, glassy microspherules recovered from Chinese loess may be the right age to relate to the Australasian tektite event, perhaps as part of the impacting body. The most serious shortcomings of the commonly

Mizera, J., Řanda, Z., Suchý, V., Strunga, V., Klokočník, J., Kostelecký, J., Bezděk, A., and Moravec, Z., 2021, Parent crater for Australasian tektites beneath the sands of the Alashan Desert, Northwest China: Best candidate ever?, *in* Foulger, G.R., Hamilton, L.C., Jurdy, D.M., Stein, C.A., Howard, K.A., and Stein, S., eds., In the Footsteps of Warren B. Hamilton: New Ideas in Earth Science: Geological Society of America Special Paper 553, https://doi.org/10.1130/2021.2553(25).

accepted Indochina impact location include signs of little chemical weathering of source materials of Australasian tektites, unlike highly weathered sedimentary targets in Indochina, and questionable assumptions about transport of distal ejecta.

INTRODUCTION

The parent impact crater for Australasian tektites is still waiting for discovery, despite their occurrence over up to one sixth of Earth's surface. For several decades, the search for the crater mostly continued to focus on Southeast Asia, within or close to the densest occurrence of Australasian tektites (e.g., Schnetzler, 1992). Gradually, with ever greater risk of confirmation bias, the consensus on the impact in Indochina has become unshakable. The recently suggested location of the impact at the Bolaven volcanic field in southern Laos (Sieh et al., 2020) may have been, despite serious flaws and possibly insufficient crater size, uncritically accepted as definitive by many researchers.

This chapter argues that this consensus overlooked analogies with other tektite fields and well-known geochemical similarities of Australasian tektites to Chinese loess on one side and incompatibility of chemically weathered sediments prevailing in Indochina on the other side, and has been based on questionable assumptions of distal ejecta ballistic transport. The general incompatibility of an Indochina location in the quest for the Australasian tektite parent crater has been pointed out by Mizera et al. (2016), who proposed an alternative hypothesis locating the source to the Badain Jaran Desert (or possibly the Tengger Desert) in Northwest China (see Fig. 1). The hypothesis indicated geochemically and isotopically more suitable source materials in that region than in Indochina, and ideal conditions for burial of the crater under Earth's largest megadunes. Geochemical, isotopic, and geographical constraints in support of that hypothesis are here elaborated along with gravity and paleoenvironmental evidence, and discussion of ballistic issues for the ejecta transport. Further, the association of glassy microspherules recovered from Chinese loess with the Australasian impact (e.g., Li et al., 1996) is revisited based on their recent dating to an age compatible with the Australasian tektite event, which is 788.1 ± 2.8 ka (Jourdan et al., 2019). The following discussion of each issue also includes a brief rebuttal of Indochina as the impact site.

GEOLOGICAL SETTING OF THE ALASHAN DESERT

The Badain Jaran Desert and Tengger Desert are the main parts of the Alashan Desert, situated on the Alxa (Alashan) Plateau in Northwest to north-central China, in the western part of

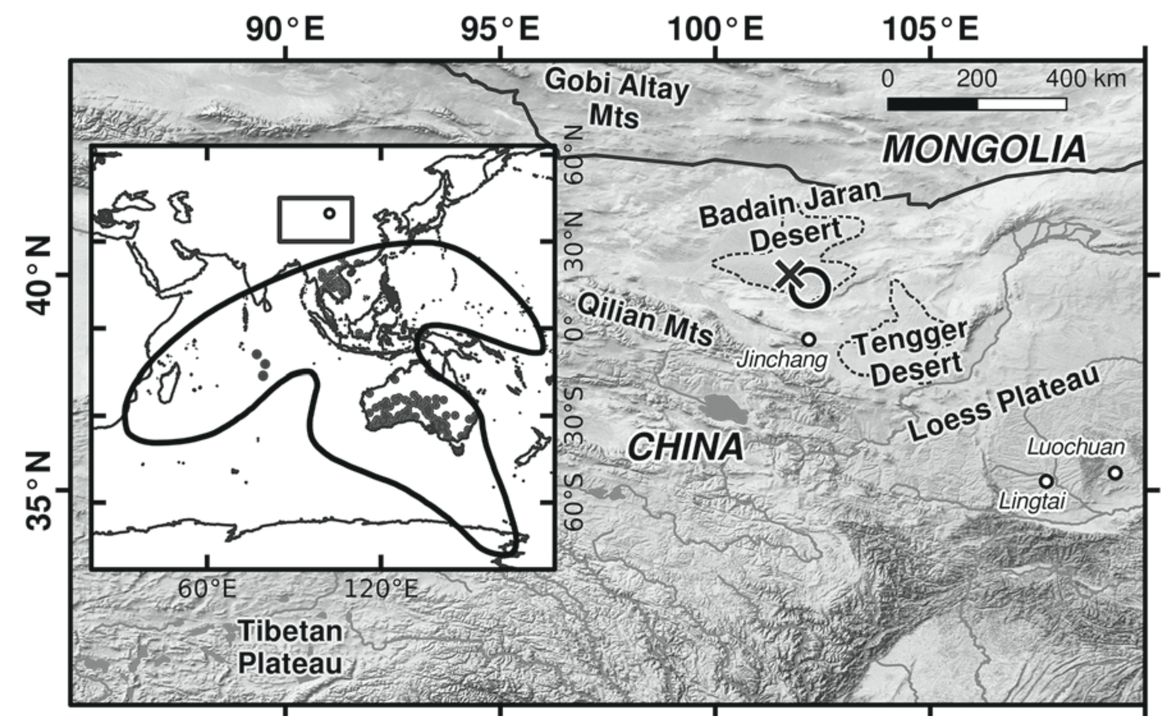

Figure 1. Hypothetical location of the parent crater for Australasian tektites (AAT) in the Badain Jaran Desert (empty circle). Cross indicates the position of the WEDP02 drill core. Inset map shows mutual position of the impact area and the entire Australasian tektite strewn field with the boundary defined by microtektite occurrences in the ocean. Full gray circles indicate macrotektite finds on land and in the Indian Ocean.

the Inner Mongolia Autonomous Region and the northern part of Gansu Province (Fig. 1). The brief geological setting presented here focuses on the Badain Jaran Desert as the main candidate for location of the hypothetical Australasian tektite source crater. Wang et al. (2015) provided detailed information on Badain Jaran Desert geology, including geologic maps, topographic profiles, and stratigraphic-lithologic charts with chronology from optically stimulated luminescence (OSL) and electron spin resonance (ESR) dating.

Badain Jaran Desert, the second largest desert in China with area of 49,000 km^2, is located in the western part of the Alxa Plateau and in the southeastern part of the Badain Jaran Basin (39.5°N–42°N, 99.5°E–103°E). Elevation roughly ranges from 900 to 1500 m above mean sea level. Boundaries of the Badain Jaran Desert are formed to the north by the Mongolian Plateau, to the south by branches and foothills of the Qilian Mountains, to the west by the alluvial/lacustrine plain of the Heihe River, and to the east by the Yabulai Mountains and Zongnai Mountains. Adjacent mountains discontinuously expose older Cenozoic and Mesozoic strata totaling as much as >2000 m thick that partially project under the Holocene dune field that forms the desert. In the southeastern part of Badain Jaran Desert, the tallest sand dunes on Earth (up to 480 m high, 3–5 km long) are interspersed with hyposaline to hypersaline and alkaline lakes. Formation and maintenance of the megadunes and recharge of the lakes probably depend on supply of deep groundwater from the adjacent fracture zone in the mountain area southeast of Badain Jaran Desert (Dong et al., 2016). Sublacustrine carbonate spring mounds and thermogenic travertine formed by seepage of deep-circulating Ca^{2+}-rich groundwater through rock fractures are found in Badain Jaran Desert and Tengger Desert (Arp et al., 1998; Dong et al., 2016). Similar rocks are known from the Ries impact structure and may be related to postimpact hydrothermal activity (Arp et al., 1998, 2013). There is a general consensus that Badain Jaran Desert represents a major source area of Chinese loess (Chen et al., 2007; Zhang et al., 2018). Badain Jaran Desert lies in a boundary region between the Westerlies and the Asian summer monsoon, and the dominating northwesterly winter monsoon is responsible for the dust transport.

GEOCHEMISTRY OF AUSTRALASIAN TEKTITES, LOESS, AND ALASHAN DESERT SEDIMENTS

The geochemical, isotopic, and age matches between tektites and their potential source materials are considered to be strong evidence in assigning a parent impact structure. The task may be complicated by a stratigraphically or horizontally complex target due to partial homogenization of geochemically diverse materials during tektite formation. The original target heterogeneity is, however, preserved to some degree in tektites and may contribute to identifying source materials and constraining impact location. In Australasian tektites, a lithological source with a small compositional variation or extreme homogenization is indicated by, e.g., homogeneous $^{143}Nd/^{144}Nd$ ratios (discussed below). Some Australasian tektites (layered, Muong Nong–type tektites), however, display significant compositional variability on regional, local, and individual sample scales, e.g., up to 20 wt% variation in SiO_2 content (Schnetzler, 1992; Skála et al., 2018). Even greater variability can be observed in microtektites, but those must have been subject to significant vapor fractionation processes, which is problematic for unambiguous source material assignment. On the other hand, potential incorporation of the impactor material is quite small to negligible. A chondritic component has been estimated by Goderis et al. (2017) at 0.5%–1% based on Ir contents, and by Ackerman et al. (2019) at up to ~0.005% based on Re-Os isotope systematics. Estimates by Folco et al. (2018) of up to 5% component based on Cr, Co, and Ni ratios may be overestimated (Schmidt, 2018).

Despite the chemical similarity of Australasian tektites to loess and other crustal materials, there are noticeable differences, including contents of some alkali and alkaline earth metals, due to sedimentary differentiation and chemical weathering. A good match for a model rock mixture with an average tektite, as well as similar compositional variations, should be observed in a target in both the vertical and horizontal directions, to a suitable depth, and over a suitably large area. Obtaining pre-impact materials is an unrealistic task, since they do not exist anymore. Mizera and Řanda (this volume) compared moldavites with pre-impact sediments near the Ries crater. Though of a proper age, they may only be an approximation due to the changes they have undergone since deposition. Modern sediments, including the soil and vegetation cover, may be compositionally closer to the original target.

Chemical Compositions

In Mizera et al. (2016), the hypothetical origin of Australasian tektites in the Alashan Desert was supported by the geochemical similarity of Australasian tektites with Chinese loess. The analyzed representative Australasian tektite suite covered all main morphological types—splash-form, layered (Muong Nong), and ablated (flanged button australites)—and major parts of the Australasian tektite strewn field (Indochina, South China, Philippines, Indonesia, Australia). Chemical comparisons in Figure 2 expand on data presented in Mizera et al. (2016), as detailed in the Supplemental Material.[1]

The compositions of Australasian tektites and loess as compared in Figure 2 are very similar with regard to their internal variability and analytical uncertainty, except for volatile elements Zn, As, Br, and Sb, which likely would be depleted during the tektite formation process, and W and Ni, which possibly were vaporized as volatile carbonyls, hydroxides, or halide compounds (Řanda et al., 2008; Žák et al., 2016, 2019). In microtektites (particularly the high-Mg group), depletion in volatile elements is even more pronounced, with alkali metals and U being strongly depleted.

[1]Supplemental Material. Samples and methods, data for Figures 2 and 3. Please visit https://doi.org/10.1130/SPE.S.16632640 to access the supplemental material, and contact editing@geosociety.org with any questions.

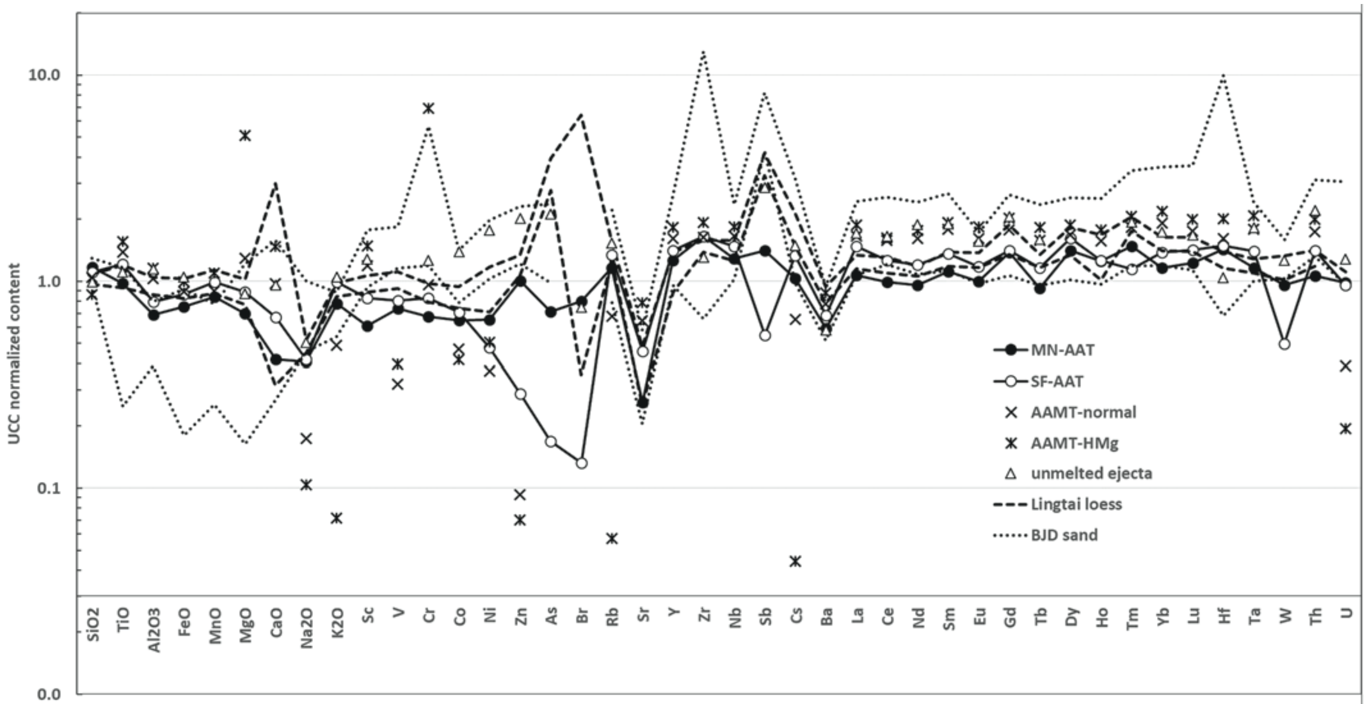

Figure 2. Average geochemical compositions of the splash-form Australasian tektites (SF-AAT; including ablated splash-form Australasian tektites), Muong Nong Australasian tektites (MN-AAT), normal and high-Mg Australasian microtektites (AAMT), and unmelted ejecta recovered from the Australasian microtektite layer in the South China Sea, compared with composition range of Lingtai loess and Badain Jaran Desert (BJD) sand. Data sources: Zhu et al. (2000); this work (Lingtai loess); Mizera et al. (2016); Žák et al. (2019) (AAT); Glass et al. (2004); Glass and Koeberl (2006); Folco et al. (2009, 2016) (AAMT); Glass and Koeberl, 2006 (unmelted ejecta); Gao et al. (2006); Hu and Yang (2016); Zhang et al. (2018); Zhao et al. (2019) (Badain Jaran Desert sand). Data are normalized to the average upper continental crust (UCC) composition adopted from Rudnick and Gao (2003). See the Supplemental Material for details (text footnote 1).

Chinese loess shows a greater range of Ca and Br contents, probably due to different carbonate contents in loess versus paleosol and anthropogenic input in the uppermost layer, respectively. The Badain Jaran Desert sand data show greater composition ranges due to a great variability of carbonate and silicate fractions, which depend strongly on grain size. The range covers compositions of loess and Australasian tektites/unmelted ejecta, but on average, the modern Badain Jaran Desert sands generally show lower Al, Fe, K/Na, and Mg/Ca values than Australasian tektites and loess. This points to a lower degree of chemical weathering in the desert sands.

For quantitative evaluation of the chemical weathering intensity (feldspar to clay conversion), the chemical index of alteration (CIA) is used, which is defined as 100 × $Al_2O_3/(Al_2O_3$ + CaO* + Na_2O + K_2O) (molar contents; where CaO* is CaO in the silicate fraction). In Australasian tektites, CIA values calculated from data in Mizera et al. (2016), assuming the indistinguishable CaO* equal to Na_2O (McLennan, 1993), range from 59 to 66, which indicate a weakly weathered target. If volatile alkali metals are depleted in Australasian tektites, the target CIA should be lower, indicating even less weathered sediments. The range in sands coeval with the impact recovered from the WEDP01 drill core in Tengger Desert is close to CIA ~60–65, contrary to CIA <55 in modern Tengger Desert sands (Li et al., 2018). The old sands also match Al and Fe contents in Australasian tektites better than modern sands.

The gradual increase in chemical weathering with decreasing latitude from North China to South China and Indochina, reflected by increasing CIA, is due to the combined monsoon climate effect on temperature and precipitation (Shao et al., 2012). We interpret the high degree of weathering to disqualify Indochina as a suitable impact location. Although some of the Mesozoic sandstones and mudstones in Indochina are geochemically similar to Australasian tektites, they bear signs of much stronger weathering, indicated by CIA >75 (Saminpanya et al., 2014), as do the strongly weathered sediments (saprolite, laterite) considered as a source component by Sieh et al. (2020). In Indochina, Australasian tektites are often found atop an upper horizon of a laterite profile, indicating that their fall coincided with the late stage of a short laterization period (Trnka, 2019). Some sandy quartz-rich sediments of the Red River in Vietnam have CIA <65 (Clift et al., 2008), but their occurrence is too sporadic to represent a sufficiently abundant target. Also, the sparse and scanty loess-like deposits found in Indochina, considered by some authors as either the source of Australasian tektites or dust ejecta ("catastroloess"), have to be disregarded. They are much younger, formed probably during the last glacial cycle (Mizera et al., 2016, and references therein). Despite climatic changes at the middle Pleistocene transition and cooling during glacial periods, Indochina was still a fairly vegetated area (Woodruff, 2010; Louys and Turner, 2012), which should be reflected in higher K/Na ratios at least in some Australasian tektites, similar to moldavites (Řanda et al., 2008; Mizera and Řanda, this volume).

Radiogenic Sr-Nd-Pb Isotope Systems

The Nd-Sr isotope systematics of tektites provide valuable information in the search for their source materials. Figure 3 shows the Nd-Sr isotopic composition of Australasian tektites compared with data for their potential source materials in the Alashan Desert. A narrow range of $^{143}Nd/^{144}Nd$ ratios in Australasian tektites, with ε_{Nd} values ranging from −10.9 to −12.2, indicates a homogeneous, old crust source material, which was probably well mixed before impact. The constraints on the provenance of target materials for tektites inferred from Nd-Sr isotopes suggested by Shaw and Wasserburg (1982) clearly disqualify a mixture of sandstone with a basaltic component as suggested by Sieh et al. (2020). Mixing calculations, assuming an ε_{Nd} range of +7.6 to −0.3 for basalts in a wider area of the Cenozoic volcanic centers (Hoang Nguyen et al., 1996) and a range of −9.9 to −13.3 for sediments derived from Mesozoic sandstones (Liu et al., 2007) in Indochina, with a similar Nd content in both components, show that a basalt admixture could not exceed 10%–20%. Up to 60% has been assumed by Sieh et al. (2020). Instantaneous homogenization during impact to satisfy the narrow ε_{Nd} range in Australasian tektites also seems improbable.

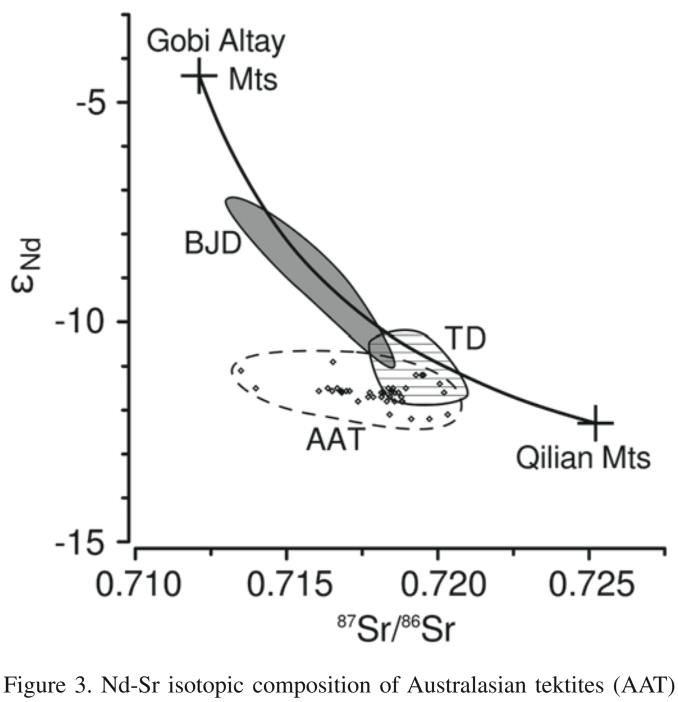

Figure 3. Nd-Sr isotopic composition of Australasian tektites (AAT) and their potential source materials in the Badain Jaran Desert (BJD) and Tengger Desert (TD). Australasian tektite data are literature values compiled from Shaw and Wasserburg (1982), Blum et al. (1992), Lee et al. (2004), and Ackerman et al. (2020). Badain Jaran Desert and Tengger Desert data are values for silicate fraction <75 µm of the desert sand (Chen et al., 2007). The mixing curve and average values for end members in the Gobi Altay Mountains and the Qilian Mountains are from Zhang et al. (2015).

A wider range in Australasian tektite $^{87}Sr/^{86}Sr$ ratios may reflect a chemically and mineralogically stratified sedimentary target with variable proportions of high $^{87}Sr/^{86}Sr$ silicate and low $^{87}Sr/^{86}Sr$ carbonate fractions. The lowest $^{87}Sr/^{86}Sr$ values in Australasian tektites belong to high-Ca australites. According to Zhang et al. (2015), the Nd-Sr isotopic pattern in the Alashan sediments represents mixing materials from two end members, the Qilian Mountains and the Gobi Altay Mountains. Due to tectonic uplift and climate change since ca. 2.7 Ma, the source has gradually been shifting from the Qilian Mountains to Gobi Altay Mountains, which is reflected in decreasing $^{87}Sr/^{86}Sr$ values and increasing ε_{Nd} values. This explains the larger variation in Nd-Sr isotopic compositions from the Badain Jaran Desert on a two-component mixing curve (see Fig. 3), and it could be consistent with an impact location in the southeastern part of Badain Jaran Desert, close to the Qilian Mountains, in agreement with the location indicated by gravity data (see below). Due to the isotopic evolution of the source of the sediments (Zhang et al., 2015), pre-impact Nd-Sr isotopic compositions in Badain Jaran Desert must have been even closer to those of Australasian tektites. On the other hand, Nd-Sr data for potential source materials in Southeast Asia, e.g., sediments from the Pearl, Red, and Mekong River basins, show greater ε_{Nd} variation (−10 to −13) and mainly $^{87}Sr/^{86}Sr$ >0.720 (Liu et al., 2007; Clift et al., 2008).

The Pb isotopic ratios based on radiogenic ^{206}Pb, ^{207}Pb, and ^{208}Pb and nonradiogenic ^{204}Pb isotopes were measured in Australasian tektites by Ackerman et al. (2020). Depletion of splash-form Australasian tektites in total Pb and ^{204}Pb compared to Muong Nong Australasian tektites indicated volatilization and isotopic fractionation of Pb. Ackerman et al. (2020) supported their preference for an Indochina impact site by the fit of Australasian tektite data within a broad range of data for sediments in the Red River drainage basin (Clift et al., 2008). The Pb isotopic ratios in Muong Nong Australasian tektites are consistent with the upper range of values observed in the Alashan Desert (Ferrat et al., 2012; Lee and Yu, 2016), or slightly higher (more radiogenic), and total Pb is slightly lower. This indicates that, if an Alashan Desert source is assumed, even Muong Nong Australasian tektites were subject to Pb loss and isotopic fractionation, though much less than splash-form Australasian tektites.

Oxygen and Other Stable Isotopes

The $\delta^{18}O$ value in quartz typically remains unchanged during diagenetic and alteration processes and is indicative of the parent rocks in which the mineral originally crystallized. Žák et al. (2019) reported that $\delta^{18}O$ values for Australasian tektites range from 8.7‰ to 11.6‰ (relative to the Vienna standard mean ocean water 2 [VSMOW2] standard) and explained the observed negative correlation between $\delta^{18}O$ and the SiO_2/Al_2O_3 ratio by variable proportions of quartz and weathered silicates in the target. Chinese loess was ruled out as a suitable source material due to a high $\delta^{18}O$ of ~16‰. However, $\delta^{18}O$ values in quartz in the Northwest China deserts are lower in coarse sand fractions than in fine dust, and $\delta^{18}O$ values down to 9.5‰ occur in sand (0.315–0.400 mm) in the area of dried lakes in Badain Jaran Desert (Yang et al., 2008). Regarding the prevalence of coarse sand in Badain Jaran Desert (0.100–0.700 mm; Wang et al., 2015), such material would have been suitable for production of Australasian tektites. One should consider an increase in $\delta^{18}O$ due to the presence of clay minerals, and a possible $\delta^{18}O$ decrease by admixture of water (meteoric and groundwater, water in hydrated minerals). Thus, to keep $\delta^{18}O$ low, a cool rather than warm climate would be preferred (Faure, 1986) for the impact area. The isotope fractionation between escaping CO_2 and the silicate melt during tektite formation may further decrease $\delta^{18}O$ (Žák et al., 2019).

Stable isotopes of other elements (K, Li, Mg, B, Cu, Zn) are less indicative of the source material provenance, although they are indispensable for understanding fractionation processes during impact and tektite formation. The isotopic fractionation of B and Li is a sensitive indicator of the continental weathering of silicates. Warm and humid conditions promote formation of weathered sediment and soil profiles characterized by significant variations in Li and B contents and isotopic compositions, usually with significant correlations among them; such features are not observed in Australasian tektites. Higher $\delta^{11}B$ values in australites compared to splash-form and Muong Nong Australasian tektites may again point to a higher carbonate content in their source (Mizera et al., 2016).

Cosmogenic Radionuclide ^{10}Be

High ^{10}Be contents in Australasian tektites (60–280 Mat/g, decay corrected) probably result from binding of the meteoric ^{10}Be to clay minerals in source materials. The observed ^{10}Be increase with distance from Indochina to Australia reflects a relation between excavation depth and the ejecta launch velocity and angle (Ma et al., 2004; Rochette et al., 2018). A thick loess (low ^{10}Be) column topped with a thin paleosol (high ^{10}Be) layer in Chinese loess/paleosol sequences could have provided a target in which ^{10}Be decreased with excavation depth. However, ^{10}Be contents in loess are twice those of Australasian tektites, and loess is too fine and homogeneous compared to mineral inclusions in Muong Nong Australasian tektites and unmelted ejecta. Also, ^{10}Be decreases with increasing Ca content in loess, opposite to the trend observed in Australasian tektites. Loess source materials in Badain Jaran Desert comply much better with Australasian tektites. Ranges of ^{10}Be—10^7 at/g in sand (0.208 mm) and 10^8 at/g in calcrete formed in the desert and dust originating from the desert (Shen et al., 2010)—correspond to Australasian tektites, although the total budget seems to be slightly lower with regard to prevalence of coarse sand in Badain Jaran Desert. This deficiency can be offset by paleoenvironmental considerations. The impact occurred 12–15 k.y. prior to the Brunhes-Matuyama geomagnetic polarity reversal, at a transition from glacial marine oxygen isotope stage (MIS) 20 to interglacial MIS 19, and at a maximum in the benthic $\delta^{18}O$ stack record. Increased precipitation, temperature, and weathering rates promoted ^{10}Be deposition in sediments. This period was also characterized by an increase in the global ^{10}Be production rate, which, at the time of impact, was at least ~30% higher than that occurring today (Simon et al., 2018). Therefore, the bulk of Badain Jaran Desert sand at the glacial-interglacial transition was partly weathered and enriched in fine dust fractions (see below) and could approximately match Australasian tektites in ^{10}Be content.

On the contrary, a model of a variably weathered (high ^{10}Be) and fresh (zero ^{10}Be) bedrock mixture, as suggested by Blum et al. (1992) and adopted by others (Rochette et al., 2018; Sieh et al., 2020), fails mainly due to mixing issues, as pointed out by Ma et al. (2004). Instantaneous homogenization during impact to obtain the relatively narrow ^{10}Be range in Australasian tektites is improbable, as with the ε_{Nd} discussion above. Moreover, a target in which the ^{10}Be content decreases monotonously with depth may not work for tropical soils, which often show deeper infiltration of meteoric ^{10}Be in otherwise uniform profiles (Graly et al., 2010).

GRAVITY DATA

A residual negative gravity anomaly over an impact crater is its most apparent geophysical signature (Pilkington and Grieve, 1992). Our inspection of the gravity data in the hypothetical target area showed the existence of a roughly circular structure centered at 39.7°N, 102.2°E, within the lake area in Badain Jaran Desert (see Fig. 4). The structure is characterized by a −100 mGal gravity anomaly with a diameter ~50 km, surrounded by a rim of ~100 km diameter with a pronounced positive gravity anomaly. The radial second derivative (T_{zz}) of the disturbing geopotential shows minima and a fragmented rim. Virtual deformations exhibit a strong compression trend. The observed gravity features are similar to analogous data for the Popigai impact structure, shown for comparison in Figure 4. Our findings from the global gravity data are consistent with ground gravity survey data in Yang et al. (2011).

PALEOENVIRONMENTAL RECONSTRUCTIONS FROM DRILL CORES IN THE ALASHAN DESERT

Wang et al. (2015) studied the formation history of the Badain Jaran Desert using data obtained from the WEDP02 drill core, a 310-m-long core at the central-southeast part of Badain Jaran Desert (40°01′N, 101°44′E), at the northwest edge of the hypothetical crater indicated by gravity data (see Figs. 1 and 4). Pre–Australasian impact lithology of the core supports supplies of a suitable source material and indicates favorable conditions for crater burial. The depth difference between the desert basal layer of alluvial/fluvial sediments at ca. 1.1 Ma (~230 m) and the layer of eolian coarse sands at the time of impact, ca. 0.8 Ma

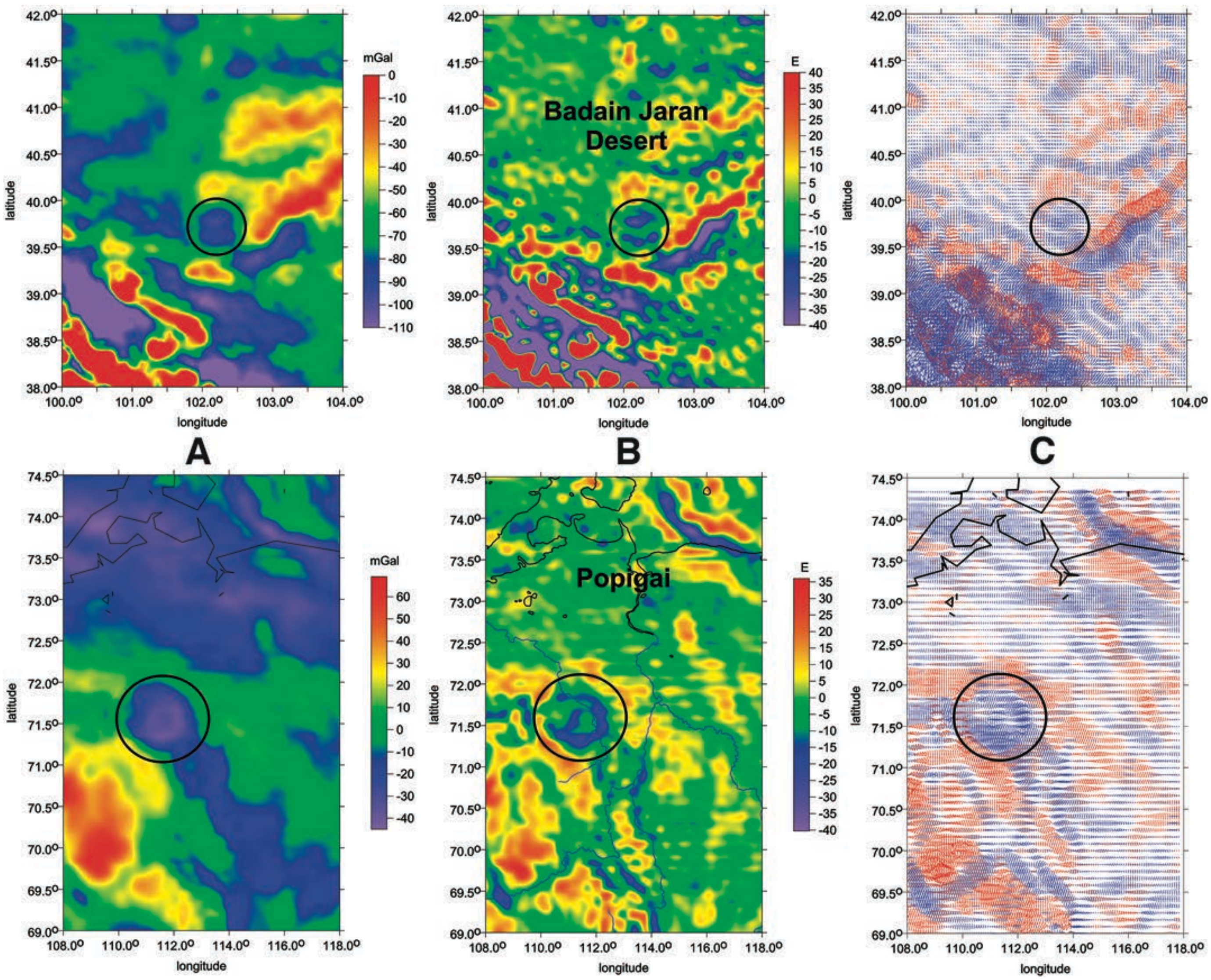

Figure 4. Gravity aspects for the hypothetical impact structure in the Badain Jaran Desert (top), compared with data for the Popigai impact structure (bottom): (A) gravity disturbances (mGal), (B) radial second derivative (T_{zz}) of the disturbing geopotential, and (C) virtual deformations (blue—compression, red—dilatation), all computed from the full static global Earth gravity field model EIGEN 6C4, with ground half-wavelength resolution of ~9 km and precision of 10 mGal (Förste et al., 2014). Coordinates: Latitude in °N, longitude in °E. For associated theory and examples of the model application in inspection of impact structures, see, e.g., Klokočník et al. (2020) and Klokočník et al. (this volume).

(~180 m), is ~50 m. The corresponding lithological unit consists of coarse sand intercalated with 5–10 cm layers of weakly carbonate-cemented coarse sand. The sand grains in the unit are loose and very well sorted and rounded (Wang et al., 2015).

Paleoenvironmental proxies in the core (sand/dust proportions, grain size, carbonate content) show that supplies of dust and carbonate fractions were higher in warmer and more humid conditions of interglacials than during glacials. The record of carbonate content in the core shows a steady increase from <0.1% at MIS 25 (ca. 950 ka, ~210 m) to ~10% at MIS 19 (ca. 790 ka, ~175 m), with several sharp turnovers due to glacial-interglacial cycling. If we assume that Ca/^{10}Be-enriched australites versus depleted Muong Nong Australasian tektites originated from the uppermost and bottom parts of the excavated target sequence, respectively, the carbonate content depth profile would constrain the Australasian tektite source materials to the ~35-m-thick column deposited about ~160 k.y. before the impact. The turnovers in the carbonate content could explain the high Ca contents in high-Ca philippinites and microtektites, which are up to 9–10 wt%, according to data compiled by Howard (2011).

The sands at ~180 m depth have a unimodal grain-size distribution (~370 µm) that is quite distinct from underlying and overlying units with trimodal to quadrimodal distributions, which could be attributed to impact fallout or a postimpact abrupt shift in the grain-size distribution—from the lofted mass of sediment with wide grain-size range, the coarse fraction fell back first to form a relatively thick layer with fine fractions absent. In the overlying unit (~160–120 m), significant changes in the proxies (dust and carbonate increase, sand decreases) indicate a transition from a desert to lake environment in Badain Jaran Desert. Despite ESR dating to 800–700 ka, this unit was stratigraphically correlated with MIS 13–15 (650–450 ka), when significant variation of the Asian monsoon occurred (stronger summer, weaker winter monsoon) as indicated by the mass accumulation rate of Chinese loess. The environmental transition to warm and humid climate is widely recorded in the Asian interior and marine records worldwide, but its cause remains unclear (Wang et al., 2015). In contrast, global climatic changes seem to contradict the paleoenvironmental record in the WEDP01 drill core in Tengger Desert (38°23′N, 104°39′E), where the decrease in CIA and Al and Fe contents indicates increasing aridification in the area since ca. 900 ka (Li et al., 2018). Could thus the lake environment formation in Badain Jaran Desert have been related to late post-impact effects, similar to the lake formation in the Ries impact structure (Arp, 2006), rather than to the global climatic changes?

Considering the position of WEDP02 core just at the edge of the proposed impact crater, a question arises on the apparent absence of signs of a proximal ejecta blanket. Although the core must not have been inspected for these unexpected features, at least some should not escape attention during analyses, and so they may really be missing (except for the possible impact fallout at ~180 m depth of the core). Impact in a highly porous target can lead to formation of a crater without ejecta deposits. Although the theory (Housen and Holsapple, 2012; Housen et al., 2018) has rather been considered for small, porous planetary bodies, porosity-related ejecta suppression has been suggested for the Marquez Dome (Buchanan et al., 1998) and Steinheim (Buchner and Schmieder, 2015) impact structures.

Impact into Badain Jaran Desert, a vast desert area surrounded downrange by high mountains, could explain its relatively small ecological consequence. Survival of hominins in South China (Wang et al., 2014) would hardly be congruent with thermal radiation from the plume produced by the Australasian impact; according to Svetsov and Shuvalov (2019), the area of fire initiation ranges from 10^6 to 10^7 km^2 for impact of a 1–3 km body, respectively.

UNMELTED EJECTA IN OCEANIC MICROTEKTITE LAYER

The shock-metamorphosed rock fragments found in the microtektite layer in the South China Sea and associated with Australasian tektites due to similar geochemistry also constrain Australasian tektite source materials. Their porosity, grain size, and mineral assemblage point to a fine-grained, quartz-rich sedimentary, loess-like source (Glass and Koeberl, 2006; Glass and Fries, 2008). Despite the 10 Å phase identified as mica/clay in some rock fragments, the abundant K-feldspar and plagioclase again indicate a weakly weathered target. Feldspars in the Cretaceous sediments in Indochina are mostly weathered to micas and kaolinite (Saminpanya et al., 2014; Uchida et al., 2010). The presence of angular to rounded grains of calcite and dolomite (probably detrital) also points to a cooler climate in the pre-impact area. In warm and humid climate, primary calcite and dolomite dissolve and form secondary (pedogenic) minerals, but secondary dolomite forms only as a protodolomite (Meng et al., 2015). In the arid area of Northwest China, dolomite is present only in the deserts on the north margin of Tibetan Plateau, including Badain Jaran Desert (Li et al., 2007). The grain size of the unmelted ejecta (<50 μm–600 μm, average 200 μm; quartz grains up to ~100 μm but mostly <50 μm) is larger than a median value of 5–40 μm for Chinese loess (Ding et al., 2002) and probably smaller than that of most Mesozoic sandstones from the Khorat Plateau at the Thailand-Laos border (Uchida et al., 2010). Grain-size analysis of sediments in the WEDP02 drill core in the Badain Jaran Desert provides two major components, eolian sand and dust, with size ranges of 100–700 μm and 2–50 μm, and proportions of 80%–100% and <20%, respectively. In the pre-impact strata, fluctuations of an increased dust proportion up to ~30% occurred (Wang et al., 2015).

"MICROTEKTITES" IN LOESS

A series of papers (e.g., Li et al., 1996) reported analyses of glassy microspherules or "microtektites" in the Luochuan loess section (35.4°N, 109.3°E; Fig. 1), accompanied by anomalous values of $\delta^{13}C$, magnetic susceptibility, and grain size of loess in the host layer, with elevated levels of Cr, Co, Mo, Hf, Ta, Sc, and As. Association of the "microtektites" with the Australasian impact was doubted due to their position above the Brunhes-Matuyama reversal (the impact preceded the Brunhes-Matuyama reversal [see above]) and their major oxide composition, which was dissimilar from Australasian tektites (Glass and Simonson, 2013). However, in Chinese loess, the Brunhes-Matuyama reversal occurs ~25 k.y. prior to the age found in marine sediments, probably due to postdepositional magnetic overprinting of loess. Using ^{10}Be as a proxy for global average geomagnetic field intensity, Zhou et al. (2014) showed that the pronounced minimum in field intensity required for the reversal is recorded in loess synchronous with Brunhes-Matuyama reversal timing in marine records. The position of the "microtektite" layer may thus be coincident with the impact.

The composition of these "microtektites" is indeed quite different from most Australasian tektites, but some glassy Si-Mg microspherules have forsterite/enstatite-like compositions. Their origin from impactor ablation was suggested by Li et al. (1996) but doubted by Glass and Simonson (2013) due to their low FeO contents. Depletion of siderophile elements is known from most stony ablation spherules collected in stratosphere and deep-sea sediments (Brownlee et al., 1983), and the composition of the glassy Si-Mg microspherules is similar to low-FeO chondrules in ordinary chondrites (Krot and Wasson, 1995). Selective ablation and separation of chondrules off the matrix seem unlikely, but ordinary and enstatite chondrites comprise up to 80 vol%

chondrules, and the minor, volatile-rich matrix with dominance of metallic and sulfidic Fe (Scott and Krot, 2007) could easily volatilize. The association of the "microtektites" with Australasian tektites is thus supported by the suitable timing of their deposition and possibly extraterrestrial origin. If the anomalous features found in their host loess layer can be attributed to the impact fallout, then the impact in Northwest China seems more probable than in Indochina.

GEOGRAPHIC, BALLISTIC, AND OTHER CONSIDERATIONS

The impact location in the Badain Jaran Desert provides a triangle "fan" of Australasian tektite ejection and distribution (macrotektites only) with an apex angle of ~60° and rays delimited by locations of Australasian tektite finds in northern Thailand in the west and in the Philippines in the east. A similar angle is obtained for the westernmost finds in the Indian Ocean and the easternmost finds in Australia; the fan only rotates to west, probably due to Earth's rotation during tektite flight (for theory, see Harris, this volume). A similar fan angle is observed in the Central European tektite strewn field. The distribution of microtektites is unlikely to be purely ballistic; atmospheric and oceanic circulation (especially shortly after the impact) must have affected the positions of their final deposition, also considering the possible ablation origin of some microtektites.

The consensus location for the Australasian impact directly inside the tektite strewn field in Indochina is not common in other known tektite strewn fields. Tektites should not be found in the immediate vicinity of the crater (except for tektite-like irghizites, which are fallback ejecta from the Zhamanshin crater; Mizera et al., 2012) or even far uprange (in the direction from which the impactor arrived); see Artemieva (2002) for theory. That factor weakens any Indochina origin hypothesis for the northernmost Australasian tektites in South China, which are several crater diameters distant from Indochina. The layered Muong Nong Australasian tektites should not be confused with the proximal ejecta. In other tektite strewn fields, occurrence of Muong Nong–type tektites is rare, and these are still found at considerable (downrange) distances from their parent craters: Muong Nong moldavites are at ~12–13 crater diameters from the Ries crater, and the Muong Nong georgiaite is at 9–19 diameters from the Chesapeake Bay impact structure, considering its uncertain diameter (Glass, 2000; Deutsch and Koeberl, 2006). We explain the occurrence of Muong Nong Australasian tektites in a limited, relatively small area by ejection of tektite melt in separate expanding jets. Muong Nong Australasian tektites represent a jet lying on the axis of the strewn field fan, i.e., in the direction from which the impactor arrived (and from which the highest momentum was imparted). The Muong Nong Australasian tektite jet is more focused (less expanding) because of the higher mass of individual tektite bodies, i.e., higher inertia, and possibly also because of higher viscosity of the melt (more resistance to splitting into droplets by shear).

Disqualifying Chinese loess from potential source materials for Australasian tektites because of too large a distance (over 2000 km), which the largest and heaviest Muong Nong Australasian tektites would have traveled, between the Chinese Loess Plateau and Indochina, as proposed by Blum et al. (1992), has no ballistic justification. The ballistic coefficient (a measure of ability to overcome air resistance in flight) of bodies with the same density and shape is directly proportional to their size. Much smaller (ablated) splash-form Australasian tektites traveled several times farther. If objects move without drag, their flight range depends on their launch velocity and angle only, not size (mass). Moving the impact location from Indochina some 2000 km to the north does not change interpretations of the distribution of various morphological and constitutional Australasian tektite types, microtektites, unmelted ejecta, and high-pressure phases; the Indochina part of the Australasian tektite strewn field still remains nearest to the parent crater. The large distance traveled by Australasian tektites seems to be incompatible with the absence of aerodynamic ablation on the bodies of Muong Nong Australasian tektites and most splash-form Australasian tektites, and with the presence of relict mineral grains including high-pressure phases in Muong Nong Australasian tektites. However, ablative effects may be reduced by factors such as tektite size, shape, and rotation. According to Chapman and Larson (1963), whose calculations and laboratory experiments reproduced flanged buttons, the conspicuous ablation flange can only form on a tektite of a sufficiently regular primary shape flying at a fixed orientation. On irregular shapes turning during ablation, heating is spread around the circumference, with little or possibly no glass removed from the original contour. The blurred aerodynamic record becomes further clouded after 788 k.y. of exposure to tropical corrosion (contrary to flanged buttons resting in the dry Australian climate). Sepri et al. (1981) explained reduced ablation by swarming reentry, where trailing particles encounter a less severe thermal loading pulse. Further, the relation between the degree of shock metamorphism/formation temperature-pressure and distance traveled may provide information on the relative distance traveled by tektites within a single impact/strewn field, not the absolute distance traveled. Speculations on distances traveled by tektites (Glass, 2000) or restriction of the Australasian impact to an area centered over Southeast Asia (Cavosie et al., 2018) by the degree of shock metamorphism would require a model relating temperature-pressure experienced by the prototektites to their launch velocity and angle.

In the case of an alternative location offshore Indochina, in the South China Sea, the impact would again hit quite weathered target sediments with CIA values mostly >70 (Clift et al., 2014). Additionally, an impact structure would not likely be overlooked in geophysical prospecting for gas and oil resources (Lei et al., 2015; Lei and Clift, 2019, personal commun.), nor would the geological, geohydrological, and geographical consequences known, for example, from the Chesapeake Bay impact associated with the smaller North American tektite strewn field (Poag, 1997). Australasian tektite geochemistry also does not support their origin in a marine environment, contrary to North American tektites, for which the B isotopic compositions and enrichment in Na may indicate a marine target (Deutsch and Koeberl, 2006). Ackerman et al. (2019) speculated that elevated contents of halogens in Muong Nong Australasian tektites (data by Koeberl, 1992) indicate a saline character of the pore water in the target rock. However, those data testify against seawater admixture: Cl and Na are anticorrelated, and high Br/Cl ratios (0.005–0.028 vs. 0.0035 in seawater) increase with increasing Cl.

CONCLUSIONS

Several strong and independent lines of evidence support a location of the parent impact crater for Australasian tektites in the Alashan Desert in Northwest China. These lines of evidence include geochemical and isotopic, geographic, paleoenvironmental, and ballistic comparisons and considerations, favorable supply and burial conditions, existence of a circular gravity anomaly, and likely association of glassy microspherules in Chinese loess with the Australasian impact. The proposed location of the Australasian impact crater in Northwest China may surpass the ubiquitously accepted Indochina location principally in the issues of chemical weathering of source materials and transport of distal ejecta.

ACKNOWLEDGMENTS

Funding was provided by the MEYSCR projects CZ.02.1.01/0.0/0.0/16_019/0000728, LTT18011, and LO1506, and Astronomical Institute, Czech Academy of Sciences institutional support program RVO 67985815. We thank Jan Kameník for help with preparation of figures, Keith Howard and Nancy Riggs for editorial handling, Kieren T. Howard and an anonymous reviewer for their valuable comments, and Thomas H.S. Harris for challenging discussions and language editing.

REFERENCES CITED

Ackerman, L., Skála, R., Křížová, Š., Žák, K., and Magna, T., 2019, The quest for an extraterrestrial component in Muong Nong–type and splash-form Australasian tektites from Laos using highly siderophile elements and Re-Os isotope systematics: Geochimica et Cosmochimica Acta, v. 252, p. 179–189, https://doi.org/10.1016/j.gca.2019.03.009.

Ackerman, L., Žák, K., Skála, R., Rejšek, J., Křížová, Š., Wimpenny, J., and Magna, T., 2020, Sr-Nd-Pb isotope systematics of Australasian tektites: Implications for the nature and composition of target materials and possible volatile loss of Pb: Geochimica et Cosmochimica Acta, v. 276, p. 135–150, https://doi.org/10.1016/j.gca.2020.02.025.

Arp, G., 2006, Sediments of the Ries Crater Lake (Miocene, Southern Germany): https://goescholar.uni-goettingen.de/bitstream/handle/1/3181/Exkursionsfuehrer-Sediment2006-Ries.pdf (accessed March 2020).

Arp, G., Hofmann, J., and Reitner, J., 1998, Microbial fabric formation in spring mounds (“microbialites”) of alkaline salt lakes in the Badain Jaran Sand Sea, PR China: Palaios, v. 13, p. 581–592, https://doi.org/10.2307/3515349.

Arp, G., Kolepka, C., Simon, K., Karius, V., Nolte, N., and Hansen, B.T., 2013, New evidence for persistent impact-generated hydrothermal activity in the Miocene Ries impact structure, Germany: Meteoritics & Planetary Science, v. 48, p. 2491–2516, https://doi.org/10.1111/maps.12235.

Artemieva, N.A., 2002, Tektite origin in oblique impacts: Numerical modeling of the initial stage, *in* Plado, J., and Pesonen, L.J., eds., Impacts in Precambrian Shields: Berlin, Springer, p. 257–276, https://doi.org/10.1007/978-3-662-05010-1_10.

Blum, J.D., Papanastassiou, D.A., Koeberl, C., and Wasserburg, G.J., 1992, Nd and Sr isotopic study of Australasian tektites: New constraints on the provenance and age of target materials: Geochimica et Cosmochimica Acta, v. 56, p. 483–492, https://doi.org/10.1016/0016-7037(92)90146-A.

Brownlee, D.E., Bates, B., and Beauchamp, R.H., 1983, Meteor ablation spherules as chondrule analogs, *in* King, E.A., ed., Chondrules and Their Origin: Houston, Texas, Lunar and Planetary Institute, p. 10–25.

Buchanan, P.C., Koeberl, C., and Reid, A.M., 1998, Impact into unconsolidated, water-rich sediments at the Marquez Dome, Texas: Meteoritics & Planetary Science, v. 33, p. 1053–1064, https://doi.org/10.1111/j.1945-5100.1998.tb01712.x.

Buchner, E., and Schmieder, M., 2015, The Steinheim Basin impact crater (SW-Germany)—Where are the ejecta?: Icarus, v. 250, p. 529–543, https://doi.org/10.1016/j.icarus.2014.12.026.

Cavosie, A.J., Timms, N.E., Erickson, T.M., and Koeberl, C., 2018, New clues from Earth’s most elusive impact crater: Evidence of reidite in Australasian tektites from Thailand: Geology, v. 46, p. 203–206, https://doi.org/10.1130/G39711.1.

Chapman, D.R., and Larson, H.K., 1963, On the lunar origin of tektites: Journal of Geophysical Research, v. 68, p. 4305–4358, https://doi.org/10.1029/JZ068i014p04305.

Chen, J., Li, G., Yang, J., Rao, W., Lu, H., Balsam, W., Sun, Y., and Ji, J., 2007, Nd and Sr isotopic characteristics of Chinese deserts: Implications for the provenances of Asian dust: Geochimica et Cosmochimica Acta, v. 71, p. 3904–3914, https://doi.org/10.1016/j.gca.2007.04.033.

Clift, P.D., Long, H.V., Hinton, R., Ellam, R.M., Hannigan, R., Tan, M.T., Blusztajn, J., and Duc, N.A., 2008, Evolving East Asian river systems reconstructed by trace element and Pb and Nd isotope variations in modern and ancient Red River–Song Hong sediments: Geochemistry Geophysics Geosystems, v. 9, Q04039, https://doi.org/10.1029/2007GC001867.

Clift, P.D., Wan, S., and Blusztajn, J., 2014, Reconstructing chemical weathering, physical erosion and monsoon intensity since 25 Ma in the northern South China Sea: A review of competing proxies: Earth-Science Reviews, v. 130, p. 86–102, https://doi.org/10.1016/j.earscirev.2014.01.002.

Deutsch, A., and Koeberl, C., 2006, Establishing the link between the Chesapeake Bay impact structure and the North American tektite strewn field: The Sr-Nd isotopic evidence: Meteoritics & Planetary Science, v. 41, p. 689–703, https://doi.org/10.1111/j.1945-5100.2006.tb00985.x.

Ding, Z.L., Derbyshire, E., Yang, S.L., Yu, Z.W., Xiong, S.F., and Liu, T.S., 2002, Stacked 2.6-Ma grain size record from the Chinese loess based on five sections and correlation with the deep-sea $\delta^{18}O$ record: Paleoceanography, v. 17, p. 5-1–5-21, https://doi.org/10.1029/2001PA000725.

Dong, Z., Wang, N., Chen, J., Li, Z., Chen, H., Chen, L., and Ma, N., 2016, New observational and experimental evidence for the recharge mechanism of the lake group in the Alxa Desert, north-central China: Journal of Arid Environments, v. 124, p. 48–61, https://doi.org/10.1016/j.jaridenv.2015.07.008.

Faure, G., 1986, Principles of Isotope Geology (2nd ed.): New York, John Wiley & Sons, 608 p.

Ferrat, M., Weiss, D.J., Dong, S., Large, D.J., Spiro, B., Sun, Y., and Gallagher, K., 2012, Lead atmospheric deposition rates and isotopic trends in Asian dust during the last 9.5 kyr recorded in an ombrotrophic peat bog on the eastern Qinghai–Tibetan Plateau: Geochimica et Cosmochimica Acta, v. 82, p. 4–22, https://doi.org/10.1016/j.gca.2010.10.031.

Folco, L., D’Orazio, M., Tiepolo, M., Tonarini, S., Ottolini, L., Perchiazzi, N., Rochette, P., and Glass, B.P., 2009, Transantarctic Mountain microtektites: Geochemical affinity with Australasian microtektites: Geochimica et Cosmochimica Acta, v. 73, p. 3694–3722, https://doi.org/10.1016/j.gca.2009.03.021.

Folco, L., D’Orazio, M., Gemelli, M., and Rochette, P., 2016, Stretching out the Australasian microtektite strewn field in Victoria Land Transantarctic Mountains: Polar Science, v. 10, p. 147–159, https://doi.org/10.1016/j.polar.2016.02.004.

Folco, L., Glass, B.P., D’Orazio, M., and Rochette, P., 2018, Australasian microtektites: Impactor identification using Cr, Co and Ni ratios: Geochimica et Cosmochimica Acta, v. 222, p. 550–568, https://doi.org/10.1016/j.gca.2017.11.017.

Förste, C., Bruinsma, S.L., Abrikosov, O., Lemoine, J.M., Marty, J.C., Flechtner, F., Balmino, G., Barthelmes, F., and Biancale, R., 2014, EIGEN-6C4: The latest combined global gravity field model including GOCE data up to degree and order 2190 of GFZ Potsdam and GRGS Toulouse: Geophysical Research Abstracts, v. 16, p. EGU2014-EGU3707, https://doi.org/10.5880/ICGEM.2015.1.

Gao, Q., Tao, Z., Li, B., Jin, H., Zou, X., Zhang, Y., and Dong, G., 2006, Palaeomonsoon variability in the southern fringe of the Badain Jaran Desert, China, since 130 ka BP: Earth Surface Processes and Landforms, v. 31, p. 265–283, https://doi.org/10.1002/esp.1242.

Glass, B.P., 2000, Relict zircon inclusions in Muong Nong–type Australasian tektites: Implications regarding the location of the source crater: Houston, Texas, Lunar and Planetary Institute, Lunar and Planetary Science Conference XXXI, p. 1196.

Glass, B.P., and Fries, M., 2008, Micro-Raman spectroscopic study of fine-grained, shock-metamorphosed rock fragments from the Australasian microtektite layer: Meteoritics & Planetary Science, v. 43, p. 1487–1496, https://doi.org/10.1111/j.1945-5100.2008.tb01023.x.

Glass, B.P., and Koeberl, C., 2006, Australasian microtektites and associated impact ejecta in the South China Sea and the middle Pleistocene supereruption of Toba: Meteoritics & Planetary Science, v. 41, p. 305–326, https://doi.org/10.1111/j.1945-5100.2006.tb00211.x.

Glass, B.P., and Simonson, B.M., 2013, Distal Impact Ejecta Layers: A Record of Large Impacts in Sedimentary Deposits: Berlin, Springer, 716 p., https://doi.org/10.1007/978-3-540-88262-6.

Glass, B.P., Huber, H., and Koeberl, C., 2004, Geochemistry of Cenozoic microtektites and clinopyroxene-bearing spherules: Geochimica et Cosmochimica Acta, v. 68, p. 3971–4006, https://doi.org/10.1016/j.gca.2004.02.026.

Goderis, S., Tagle, R., Fritz, J., Bartoschewitz, R., and Artemieva, N., 2017, On the nature of the Ni-rich component in splash-form Australasian tektites: Geochimica et Cosmochimica Acta, v. 217, p. 28–50, https://doi.org/10.1016/j.gca.2017.08.013.

Graly, J.A., Bierman, P.R., Reusser, L.J., and Pavich, M.J., 2010, Meteoric ^{10}Be in soil profiles—A global meta-analysis: Geochimica et Cosmochimica Acta, v. 74, p. 6814–6829, https://doi.org/10.1016/j.gca.2010.08.036.

Harris, T.H.S., 2021, this volume, Terrestrial ejecta suborbital transport and the rotating frame transform, *in* Foulger, G.R., Hamilton, L.C., Jurdy, D.M., Stein, C.A., Howard, K.A., and Stein, S., eds., In the Footsteps of Warren B. Hamilton: New Ideas in Earth Science: Geological Society of America Special Paper 553, https://doi.org/10.1130/2021.2553(23).

Hoang Nguyen, Flower, M.F.J., and Carlson, R.W., 1996, Major, trace element, and isotopic compositions of Vietnamese basalts: Interaction of hydrous EM1-rich asthenosphere with thinned Eurasian lithosphere: Geochimica et Cosmochimica Acta, v. 60, p. 4329–4351, https://doi.org/10.1016/S0016-7037(96)00247-5.

Housen, K.R., and Holsapple, K.A., 2012, Craters without ejecta: Icarus, v. 219, p. 297–306, https://doi.org/10.1016/j.icarus.2012.02.030.

Housen, K.R., Sweet, W.J., and Holsapple, K.A., 2018, Impacts into porous asteroids: Icarus, v. 300, p. 72–96, https://doi.org/10.1016/j.icarus.2017.08.019.

Howard, K.T., 2011, Volatile enhanced dispersal of high velocity impact melts and the origin of tektites: Proceedings of the Geologists' Association, v. 22, p. 363–382, https://doi.org/10.1016/j.pgeola.2010.11.006.

Hu, F., and Yang, X., 2016, Geochemical and geomorphological evidence for the provenance of aeolian deposits in the Badain Jaran Desert, northwestern China: Quaternary Science Reviews, v. 131, p. 179–192, https://doi.org/10.1016/j.quascirev.2015.10.039.

Jourdan, F., Nomade, S., Wingate, M.T.D., Eroglu, E., and Deino, A., 2019, Ultraprecise age and formation temperature of the Australasian tektites constrained by ^{40}Ar/^{39}Ar analyses: Meteoritics & Planetary Science, v. 54, p. 2573–2591, https://doi.org/10.1111/maps.13305.

Klokočník, J., Kostelecký, J., Cílek, V., and Bezděk, A., 2020, Subglacial and Underground Structures Detected from Recent Gravito-Topography Data: Newcastle upon Tyne, UK, Cambridge Scholars Publishing, 232 p.

Klokočník, J., Bezděk, A, and Kostelecký, J., 2021, this volume, The gravity field aspects for identification of cosmic impact structures on the Earth, *in* Foulger, G.R., Hamilton, L.C., Jurdy, D.M., Stein, C.A., Howard, K.A., and Stein, S., eds., In the Footsteps of Warren B. Hamilton: New Ideas in Earth Science: Geological Society of America Special Paper 553, https://doi.org/10.1130/2021.2553(21).

Koeberl, C., 1992, Geochemistry and origin of Muong Nong–type tektites: Geochimica et Cosmochimica Acta, v. 56, p. 1033–1064, https://doi.org/10.1016/0016-7037(92)90046-L.

Krot, A.N., and Wasson, J.T., 1995, Igneous rims on low-FeO and high-FeO chondrules in ordinary chondrites: Geochimica et Cosmochimica Acta, v. 59, p. 4951–4966, https://doi.org/10.1016/0016-7037(95)00337-1.

Lee, P.K., and Yu, S., 2016, Lead isotopes combined with a sequential extraction procedure for source apportionment in the dry deposition of Asian dust and non-Asian dust: Environmental Pollution, v. 210, p. 65–75, https://doi.org/10.1016/j.envpol.2015.12.010.

Lee, Y., Chen, J., Ho, K., and Juang, W., 2004, Geochemical studies of tektites from East Asia: Geochemical Journal, v. 38, p. 1–17, https://doi.org/10.2343/geochemj.38.1.

Lei, C., Ren, J., Sternai, P., Fox, M., Willett, S., Xie, X., Clift, P.D., Liao, J., and Wang, Z., 2015, Structure and sediment budget of Yinggehai–Song Hong basin, South China Sea: Implications for Cenozoic tectonics and river basin reorganization in Southeast Asia: Tectonophysics, v. 655, p. 177–190, https://doi.org/10.1016/j.tecto.2015.05.024.

Li, C., Ouyang, Z., and Lin, W., 1996, Microtektites in 0.7 Ma B.P. loess and geochemistry of the microtektite-bearing layers, *in* Pang, Z., Zhang, J., and Sun, J., eds., Advances in Solid Earth Sciences: Beijing, Science Press, p. 64–73.

Li, G., Chen, J., Chen, Y., Yang, J., Ji, J., and Liu, L., 2007, Dolomite as a tracer for the source regions of Asian dust: Journal of Geophysical Research, v. 112, D17201, https://doi.org/10.1029/2007JD008676.

Li, Z., Wang, F., Wang, X., Li, B., and Chen, F., 2018, A multi-proxy climatic record from the central Tengger Desert, southern Mongolian Plateau: Implications for the aridification of inner Asia since the late Pliocene: Journal of Asian Earth Sciences, v. 160, p. 27–37, https://doi.org/10.1016/j.jseaes.2018.03.022.

Liu, Z., Colin, C., Huang, W., Le, K.P., Tong, S., Chen, Z., and Trentesaux, A., 2007, Climatic and tectonic controls on weathering in South China and Indochina peninsula: Clay mineralogical and geochemical investigations from the Pearl, Red, and Mekong drainage basins: Geochemistry Geophysics Geosystems, v. 8, Q05005, https://doi.org/10.1029/2006GC001490.

Louys, J., and Turner, A., 2012, Environment, preferred habitats and potential refugia for Pleistocene *Homo* in Southeast Asia: Comptes Rendus Palévol, v. 11, p. 203–211, https://doi.org/10.1016/j.crpv.2011.03.003.

Ma, P., Aggrey, K., Tonzola, C., Schnabel, C., de Nicola, P., Herzog, G.F., Wasson, J.T., Glass, B.P., Brown, L., Tera, F., Middleton, R., and Klein, J., 2004, Beryllium-10 in Australasian tektites: Constraints on the location of the source crater: Geochimica et Cosmochimica Acta, v. 68, p. 3883–3896, https://doi.org/10.1016/j.gca.2004.03.026.

McLennan, S.M., 1993, Weathering and global denudation: The Journal of Geology, v. 101, p. 295–303, https://doi.org/10.1086/648222.

Meng, X., Liu, L., Balsam, W., Li, S., He, T., Chen, J., and Ji, J., 2015, Dolomite abundance in Chinese loess deposits: A new proxy of monsoon precipitation intensity: Geophysical Research Letters, v. 42, p. 10,391–10,398, https://doi.org/10.1002/2015GL066681.

Mizera, J., and Řanda, Z., 2021, this volume, Geochemical indicators of a biogenic component in source materials of moldavites, *in* Foulger, G.R., Hamilton, L.C., Jurdy, D.M., Stein, C.A., Howard, K.A., and Stein, S., eds., In the Footsteps of Warren B. Hamilton: New Ideas in Earth Science: Geological Society of America Special Paper 553, https://doi.org/10.1130/2021.2553(26).

Mizera, J., Řanda, Z., and Tomandl, I., 2012, Geochemical characterization of impact glasses from the Zhamanshin crater by various modes of activation analysis: Remarks on genesis of irghizites: Journal of Radioanalytical and Nuclear Chemistry, v. 293, p. 359–376, https://doi.org/10.1007/s10967-012-1673-6.

Mizera, J., Řanda, Z., and Kameník, J., 2016, On a possible parent crater for Australasian tektites: Geochemical, isotopic, geographical and other constraints: Earth-Science Reviews, v. 154, p. 123–137, https://doi.org/10.1016/j.earscirev.2015.12.004.

Pilkington, M., and Grieve, R.A.F., 1992, The geophysical signature of terrestrial impact craters: Reviews of Geophysics, v. 30, p. 161–181, https://doi.org/10.1029/92RG00192.

Poag, C.W., 1997, The Chesapeake Bay bolide impact: A convulsive event in Atlantic Coastal Plain evolution: Sedimentary Geology, v. 108, p. 45–90, https://doi.org/10.1016/S0037-0738(96)00048-6.

Řanda, Z., Mizera, J., Frána, J., and Kučera, J., 2008, Geochemical characterization of moldavites from a new locality, the Cheb Basin, Czech

Republic: Meteoritics & Planetary Science, v. 43, p. 461–477, https://doi.org/10.1111/j.1945-5100.2008.tb00666.x.

Rochette, P., Braucher, R., Folco, L., Horng, C.S., Aumaître, G., Bourlès, D.L., and Keddadouche, K., 2018, ^{10}Be in Australasian microtektites compared to tektites: Size and geographic controls: Geology, v. 46, p. 803–806, https://doi.org/10.1130/G45038.1.

Rudnick, R.L., and Gao, S., 2003, 3.01—Composition of the continental crust, *in* Holland, H.D., and Turekian, K.K., eds., Treatise on Geochemistry, Volume 3: Oxford, UK, Elsevier-Pergamon, p. 1–64, https://doi.org/10.1016/B0-08-043751-6/03016-4.

Saminpanya, S., Duangkrayom, J., Jintasakul, P., and Hanta, R., 2014, Petrography, mineralogy and geochemistry of Cretaceous sediment samples from western Khorat Plateau, Thailand, and considerations on their provenance: Journal of Asian Earth Sciences, v. 83, p. 13–34, https://doi.org/10.1016/j.jseaes.2014.01.007.

Schmidt, G., 2018, Misleading projectile determination by Cr/Ni and Ni/Co ratios of Australasian microtektites and impact melt rocks: European Planetary Science Congress Abstracts, v. 12, EPSC2018-102-9.

Schnetzler, C.C., 1992, Mechanism of Muong Nong–type tektite formation and speculation on the source of Australasian tektites: Meteoritics, v. 27, p. 154–165, https://doi.org/10.1111/j.1945-5100.1992.tb00743.x.

Scott, E.R.D., and Krot, A.N., 2007, 1.07—Chondrites and their components, *in* Holland, H.D., and Turekian, K.K., eds., Treatise on Geochemistry, Volume 1: Oxford, UK, Elsevier-Pergamon, p. 1–72, https://doi.org/10.1016/B0-08-043751-6/01145-2.

Sepri, P., Chen, K.K., and O'Keefe, J.A., 1981, Diminished tektite ablation in the wake of a swarm: Journal of Geophysical Research, v. 86, p. 5103–5111, https://doi.org/10.1029/JB086iB06p05103.

Shao, J., Yang, S., and Li, C., 2012, Chemical indices (CIA and WIP) as proxies for integrated chemical weathering in China: Inferences from analysis of fluvial sediments: Sedimentary Geology, v. 265–266, https://doi.org/10.1016/j.sedgeo.2012.03.020.

Shaw, H.F., and Wasserburg, G.J., 1982, Age and provenance of the target materials for tektites and possible impactites as inferred from Sm-Nd and Rb-Sr systematics: Earth and Planetary Science Letters, v. 60, p. 155–177, https://doi.org/10.1016/0012-821X(82)90001-2.

Shen, C.D., Beer, J., Kubik, P.W., Sun, W.D., Liu, T.S., and Liu, K.X., 2010, ^{10}Be in desert sands, falling dust and loess in China: Nuclear Instruments & Methods in Physics Research. Section B, Beam Interactions with Materials and Atoms, v. 268, p. 1050–1053, https://doi.org/10.1016/j.nimb.2009.10.095.

Sieh, K., Herrin, J., Jicha, B., Schonwalder Angel, D., Moore, J.D.P., Banerjee, P., Wiwegwin, W., Sihavong, V., Singer, B., Chualaowanich, T., and Charusiri, P., 2020, Australasian impact crater buried under the Bolaven volcanic field, southern Laos: Proceedings of the National Academy of Sciences of the United States of America, v. 117, p. 1346–1353, https://doi.org/10.1073/pnas.1904368116.

Simon, Q., Thouveny, N., Bourlès, D.L., Bassinot, F., Savranskaia, T., and Valet, J.P., 2018, Increased production of cosmogenic ^{10}Be recorded in oceanic sediment sequences: Information on the age, duration, and amplitude of the geomagnetic dipole moment minimum over the Matuyama-Brunhes transition: Earth and Planetary Science Letters, v. 489, p. 191–202, https://doi.org/10.1016/j.epsl.2018.02.036.

Skála, R., Křížová, Š., Matoušková, Š., Trnka, M., and Žák, K., 2018, Variability within and between large bodies of Muong Nong–type tektites in Laos: European Planetary Science Congress Abstracts, v. 12, EPSC2018–835.

Svetsov, V., and Shuvalov, V., 2019, Thermal radiation from impact plumes: Meteoritics & Planetary Science, v. 54, p. 126–141, https://doi.org/10.1111/maps.13200.

Trnka, M., 2019, Can loess be a source material for Australasian tektites?: Houston, Texas, Lunar and Planetary Institute, 50th Lunar and Planetary Science Conference, abstract 1864, http://www.hou.usra.edu/meetings/lpsc2019/pdf/1864.pdf.

Uchida, E., Ito, K., and Shimizu, N., 2010, Provenance of the sandstone used in the construction of the Khmer monuments in Thailand: Archaeometry, v. 52, p. 550–574, https://doi.org/10.1111/j.1475-4754.2009.00505.x.

Wang, F., Sun, D., Chen, F., Bloemendal, J., Guoa, F., Li, Z., Zhang, Y., Li, B., and Wang, X., 2015, Formation and evolution of the Badain Jaran Desert, North China, as revealed by a drill core from the desert centre and by geological survey: Palaeogeography, Palaeoclimatology, Palaeoecology, v. 426, p. 139–158, https://doi.org/10.1016/j.palaeo.2015.03.011.

Wang, W., Bae, C.J., Huang, S., Huang, X., Tian, F., Mo, J., Huang, Z., Huang, C., Xie, S., and Li, D., 2014, Middle Pleistocene bifaces from Fengshudao (Bose Basin, Guangxi, China): Journal of Human Evolution, v. 69, p. 110–122, https://doi.org/10.1016/j.jhevol.2013.11.002.

Woodruff, D.S., 2010, Biogeography and conservation in Southeast Asia: How 2.7 million years of repeated environmental fluctuations affect today's patterns and the future of the remaining refugial-phase biodiversity: Biodiversity and Conservation, v. 19, p. 919–941, https://doi.org/10.1007/s10531-010-9783-3.

Yang, X., Zhang, F., Fu, X., and Wang, X., 2008, Oxygen isotopic compositions of quartz in the sand seas and sandy lands of northern China and their implications for understanding the provenances of aeolian sands: Geomorphology, v. 102, p. 278–285, https://doi.org/10.1016/j.geomorph.2008.05.007.

Yang, X., Scuderi, L., Liu, T., Paillou, P., Li, H., Dong, J., Zhu, B., Jiang, W., Jochems, A., and Weissmann, G., 2011, Formation of the highest sand dunes on Earth: Geomorphology, v. 135, p. 108–116, https://doi.org/10.1016/j.geomorph.2011.08.008.

Žák, K., Skála, R., Řanda, Z., Mizera, J., Heissig, K., Ackerman, L., Ďurišová, J., Jonášová, Š., Kameník, J., and Magna, T., 2016, Chemistry of Tertiary sediments in the surroundings of the Ries impact structure and moldavite formation revisited: Geochimica et Cosmochimica Acta, v. 179, p. 287–311, https://doi.org/10.1016/j.gca.2016.01.025.

Žák, K., Skála, R., Pack, A., Ackerman, L., and Křížová, Š., 2019, Triple oxygen isotope composition of Australasian tektites: Meteoritics & Planetary Science, v. 54, p. 1167–1181, https://doi.org/10.1111/maps.13251.

Zhang, W., Chen, J., and Li, G., 2015, Shifting material source of Chinese loess since ~2.7 Ma reflected by Sr isotopic composition: Scientific Reports, v. 5, 10235, https://doi.org/10.1038/srep10235.

Zhang, W., Zhao, J., Chen, J., Ji, J., and Liu, L., 2018, Binary sources of Chinese loess as revealed by trace and REE element ratios: Journal of Asian Earth Sciences, v. 166, p. 80–88, https://doi.org/10.1016/j.jseaes.2018.07.017.

Zhao, W., Liu, L., Chen, J., and Ji, J., 2019, Geochemical characterization of major elements in desert sediments and implications for the Chinese loess source: Science China–Earth Sciences, v. 62, p. 1428–1440, https://doi.org/10.1007/s11430-018-9354-y.

Zhou, W., Beck, J.W., Kong, X., An, Z., Qiang, X., Wu, Z., Xian, F., and Ao, H., 2014, Timing of the Brunhes-Matuyama magnetic polarity reversal in Chinese loess using ^{10}Be: Geology, v. 42, p. 467–470, https://doi.org/10.1130/G35443.1.

Zhu, R., Guo, B., Pan, Y., Liu, Q., Zeman, A., and Suchy, V., 2000, Reliability of geomagnetic secular variations recorded in a loess section at Lingtai, north-central China: Science in China, ser. D, Earth Sciences, v. 43, p. 1–9, https://doi.org/10.1007/BF02877826.

Manuscript Accepted by the Society 15 April 2021
Manuscript Published Online 21 September 2021